

1
2 Urbanization Dramatically Altered the Water Balances of a Paddy Field Dominated Basin in
3 Southern China

4 Lu Hao¹, Ge Sun^{2*}, Yongqiang Liu³, Jinhong Wan⁴, Mengsheng Qin¹, Hong Qian¹, Chong Liu⁵,
5 Jiangkun Zheng⁶, Ranjeet John⁷, Peilei Fan⁸, and Jiquan Chen⁷

6
7 1. International Center for Ecology, Meteorology, and Environment (IceMe), Jiangsu Key
8 Laboratory of Agricultural Meteorology, Nanjing University of Information Science and
9 Technology (NUIST), Nanjing 210044, China.

10 2. ***Ge Sun (Corresponding Author)**, Research Hydrologist, Eastern Forest Environmental
11 Threat Assessment Center, Southern Research Station, USDA Forest Service, Raleigh, NC
12 27606, USA. Email: gesun@ncsu.edu; Phone: (919)5159498 (O), Fax: (919)5132978

13 3. Center for Forest Disturbance Science, Southern Research Station, USDA Forest Service,
14 Athens, GA 30602, USA

15 4. China Institute of Water Resources and Hydropower Research, Beijing 100048, China.

16 5. State Key Laboratory for Information Engineering in Surveying, Mapping and Remote
17 Sensing, Wuhan University, Wuhan 430079, China.

18 6. College of Forestry, Sichuan Agricultural University, Ya'an, Sichuan, China

19 7. Center for Global Change and Earth Observations (CGCEO), and Department of
20 Geography, Michigan State University, East Lansing, MI 48823, USA.

21 8. School of Planning, Design, and Construction (SPDC) and Center for Global Change and
22 Earth Observations (CGCEO), Michigan State University, East Lansing, MI 48823, USA.
23

24 **Abstract.** Rice paddy fields provide important ecosystem services (e.g., food production, water
25 retention, carbon sequestration) to a large population globally. However, these benefits are
26 diminishing as a result of rapid environmental and socioeconomic transformations characterized by
27 population growth, urbanization, and climate change in many Asian countries. This case study
28 examined the responses of streamflow and watershed water balances to the decline of rice paddy
29 fields due to urbanization in the Qinhuai River Basin in southern China where massive
30 industrialization has occurred in the region during the past three decades. We found that
31 streamflow increased by 58% and evapotranspiration (ET) decreased by 23% during 1986-2013 as
32 a result of an increase in urban areas of three folds and reduction of rice paddy field by 27%. Both
33 highflows and lowflows increased significantly by about 28% from 2002 to 2013. The increases in
34 streamflow were consistent with the decreases in ET and leaf area index monitored by independent
35 remote sensing MODIS data. Attribution analysis based on two empirical models indicted that
36 land use/land cover change contributed about 85% of the observed increase in streamflow from
37 353 ± 287 mm yr⁻¹ during 1986-2002 to 556 ± 145 during 2003-2013. We concluded that the
38 reduction in ET was largely attributed to the cropland conversion to urban use. The effects of land
39 use change overwhelmed the effects of regional climate warming and climate variability.
40 Converting traditional rice paddy fields to urban use dramatically altered land surface conditions
41 from an artificial wetland-dominated landscape to an urban land use- dominated one, and thus was
42 considered as one of the extreme types of contemporary hydrologic disturbances. The ongoing
43 large-scale urbanization in the rice paddy-dominated regions in the humid southern China, and
44 East Asia, will likely elevate stormflow volume, aggravate flood risks, and intensify urban heat
45 island effects. Understanding the linkage between land use/landcover change and changes in

46 hydrological processes is essential for better management of urbanizing watersheds in the rice
47 paddy dominated landscape.

48 **1 Introduction**

49 Urbanization is a global phenomenon that poses profound threats to the local environment,
50 society, and culture (Foley et al., 2005; McDonald et al., 2011). The most obvious direct
51 consequence of urbanization is the altered hydrology and water balances that control the flows of
52 energy and matter in watershed ecosystems (Paul and Meyer, 2001; Sun and Lockaby, 2012). It
53 is widely known that urbanization elevates peakflow rates (Brath et al., 2006; Du et al., 2012;
54 Sun and Lockaby, 2012) as a result of increased impervious surfaces that promote quick surface
55 runoff (Dietz and Clausen, 2008; Miller et al., 2014). However, the hydrologic response to
56 urbanization is extremely variable (Jacobson, 2011; Caldwell et al., 2012) due to climatic
57 differences and land use change patterns across a watershed (Sun and Lockaby, 2012). Empirical
58 data are still lacking about changes in water balances and watershed hydrologic characteristics
59 other than stormflows, such as total flows, lowflows, and evapotranspiration (ET) (Dow and
60 DeWalle, 2000; Boggs and Sun, 2011) in different physiographic settings (Barron et al., 2013).
61 Previous studies rely heavily on simulation models (Kang et al., 1998; Kim et al., 2005, 2014;
62 Sakaguchi et al., 2014). Controversies on the magnitude and underlying mechanisms of
63 hydrologic responses to land conversion during urbanization remain in the literature (Wang et al.,
64 2009; He et al., 2009; Sun and Lockaby, 2012). In particular, data are scarce on the effects of
65 converting paddy fields to other land uses, resulting in conflicting conclusions. For example, a
66 simulation study in Taiwan suggested that rice paddy fields generated 55% lower total runoff

67 and 33% lower peakflows than dry farms (Wu et al., 1997). However, another simulation study
68 that used the HEC-HMS model for a rice paddy dominated watershed in southern China found
69 that an increase in impervious surface areas from 3% to 30% increased the peakflow rate and
70 storm volume (4-20%), but had very limited impacts on total annual flow (<6%) (Wang et al.,
71 2009; Du et al., 2011, 2012) and thus long term water balances.

72 The highly populated Yangtze River Delta (YRD) region covers about 2% of China's land
73 mass, but provides over 18% of China's Gross Domestic Product (Gu et al., 2011). The population
74 increased by almost 13% in the past decade to 156 million in 2013, and has become China's most
75 industrialized region and one of the global 'hot spots' of economic and social development. As the
76 'homes of the fish and rice', southern China's landscapes have been dominated by rice paddy
77 fields for thousands of years. The original coastal wetlands have long been ditched, drained, and
78 cultivated for growing rice and other crops. Rice paddy fields are major sources of food
79 production and offer many other ecosystem services similar to wetlands including flood retention,
80 groundwater recharge (He et al., 2009), nutrient cycling, and sequestration of greenhouse gases
81 (Tsai, 2002). One study on 10 typical rice paddies in China concluded that their ecosystem service
82 values exceed their economic values by three folds (Xiao et al., 2011). The rapid urbanization and
83 population rise under a warming climate in the YRD region has caused serious environmental and
84 resource concerns such as overdrawing and pollution of groundwater, flooding, land subsidence,
85 and urban heat islands (He et al., 2007; Gu et al., 2011). The majority of the existing studies on
86 paddy fields have focused on grain yield and irrigation with little research on the hydrologic
87 response to urbanization in paddy field-dominated landscapes (Du et al., 2011, 2012; Kim et al.,
88 2014).

89 Converting paddies to urban land use have many cascading effects on the local environments
90 (Figure 1). In particular, because rice paddy fields are rarely under water stress, the water loss or
91 actual ET is close to the potential ET (Wu et al.,1997) and has been recognized as their cooling
92 functions in regulating local climate (Xiao et al., 2011). In contrast, urban land use is generally
93 characterized by low vegetation coverage with low ET and high runoff (Sun and Lockaby, 2012).
94 Therefore, we hypothesized that converting rice paddy fields to urban areas represents the
95 maximum ET reduction possible among all common land cover change scenarios, potentially
96 resulting in disproportionately higher impacts on water balances than other land conversion
97 scenarios (e.g., converting dryland to urban uses) . Along with the increase in impervious surface
98 areas that are well known to increase stormflow, ET reduction during urbanization is likely to
99 cause large impacts on the local micro-climate, streamflow, and water quality on paddy field
100 dominated watersheds (Figure 1).

101 The overall goal of this study was to understand the processes underlining the hydrologic
102 impacts of converting rice paddy fields to urban uses. The specific objectives of this study were: 1)
103 examine how urbanization in the past decade (2000-2013) has affected the water balances and
104 hydrologic characteristics of the Qinhuai River Basin (QRB), a typical landscape of the YRD
105 (Figure 2), 2) test the hypothesis that urbanization in a paddy field dominated watershed
106 dramatically reduced ET, thus altered water balances, and 3) explore the implications of
107 urbanization for regional environmental change in southern China. In this study, we integrated
108 long-term hydro-meteorological monitoring data and remote sensing-based ET and vegetation
109 products. Multiple advanced detection techniques were used to examine trends of climate and
110 streamflow overtime and their associations with biophysical variables such as vegetation leaf area

111 index and land use dynamics.

112 **2 Methods**

113 **2.1 The Qinhuai River Basin (QRB)**

114 As one of the key tributaries of the Yangtze River, the QRB (31°34′-32°10′N, 118°39′-119°19′E)
115 has a catchment area of 2,617 km². The QRB represents a typical landscape of the lower Yangtze
116 River Delta region that is characterized as having a flat topography with natural river networks
117 severely modified, and the land uses were dominated by paddy rice fields dotted with small
118 irrigation ponds that were converted from natural wetlands over thousands of years (Figure 2). As
119 the ‘Backyard Garden’ of Nanjing City, Capital of Jiangsu Province, the QRB is gradually
120 recognized for its important ecosystem services in drought/flood prevention, crop irrigation,
121 recreation, tourism, and emergency drinking water supply to over 8 million residents. The local
122 climate is controlled by the East Asia summer monsoon (Guo et al., 2012). The multi-year mean
123 air temperature is 15.4°C. Mean air temperature (1961-2013) across the study basin has increased
124 drastically at rate of 0.44 °C/decade from 1990 to 2013 (Figure 3), suggesting an increasing trend
125 in evaporative potential during the past two decades. The mean (1986-2013) annual precipitation
126 is 1,116 mm with 75% rainfall falling during April-October (Figure 4). The observed long-term
127 mean annual streamflow (per unit of area) is about 430 mm, concentrated from June to August.
128 The QRB has seen rapid urbanization during the past decade. The urban built-up areas increased
129 from 9% (222km²) to 12% (301 km²) from 2000 to 2004, but jumped to 23% (612 km²) in 2012,
130 and the area of rice paddy fields decreased from 45% (1,188km²) of the total land area in 2000 to
131 43% (1,112 km²) in 2004, and dramatically dropped to 36% (932 km²) in 2012 (Figure 2).
132 Documents by Jiangsu Province Rural Statistics reported that rice planting area in the QRB shrank

133 more than 25% from 995 km² in 2000 to 745 km² in 2010.

134 **2.2 Land use, Climate, Streamflow, Potential ET, ET, and Leaf Area Index (LAI)**

135 We retrieved land use and land cover data for four key time periods, 2000, 2004, 2007 and 2012,
136 using Landsat TM and ETM+ images with a 30 m pixel resolution (<http://glovis.usgs.gov/>). We
137 also compared our analysis to land use and land cover data acquired for the period from 1988 to
138 2012 from other multiple sources, including published thesis and journal papers for the study basin
139 (Du et al., 2012; Chen and Du, 2014). For land use in 2010, we also used the new Finer Resolution
140 Observation and Monitoring of Global Land Cover that was created by Tsinghua University using
141 Landsat TM and ETM+ data (Gong et al., 2013). The daily meteorological data (Precipitation,
142 Radiation, Temperature, Wind Speed, and Humidity) for estimating potential ET were acquired
143 from four standard climatic stations maintained by the local meteorological bureau across the QRB
144 (Figure 2). Streamflow data with varying temporal resolutions were compiled from hydrologic
145 records for two hydrological stations, the Wuding Sluice Gate (Wuding Station thereafter) and the
146 Inner Qinhuai Sluice Gate (Inner Qinhuai Station thereafter), which controlled the outflows from
147 the Qinhuai River and backflows from the Yangtze River (Figure 2). The daily streamflow data
148 (2002-2003; 2006-2013) for the ‘flooding periods’ from May to October recorded at the Wuding
149 Station were used to characterize highflows and lowflows. The total annual streamflow discharged
150 to the Yangtze River was the sum of flows measured at the Wuding Station and the Inner Qinhuai
151 Station. Total annual streamflow data for the period of 1986-2006 were reported in Du et al. (2011)
152 and we collected daily and monthly streamflow data for other periods.

153 Potential ET (PET) represents the maximum ecosystem evapotranspiration when soil water is

154 not limited, such as the case of paddy fields. PET represents a comprehensive index of availability
155 of atmospheric evaporative energy that is controlled by radiation, temperature, humidity, and wind
156 speed. Daily PET rates were calculated using the standard FAO 56 method and were averaged
157 across the four climatic stations for the period 2000-2013 (Allen et al., 1994). The improved
158 MOD16 datasets provide consistent estimates of global actual ET at an eight-day and 1-km²
159 resolution (Mu et al., 2011). Yuan et al. (2011) reprocessed the MODIS leaf areas index (LAI)
160 datasets using the modified temporal spatial filter (mTSF) and time-series analysis with the
161 TIMESAT software (Jonsson and Eklundh, 2004) and provided reliable continuous LAI estimates
162 from 2000 to 2013. Mean monthly PET and MODIS ET rates were presented in Figure 4 along
163 with other climatic variables to contrast seasonal ET, PET, and P that controlled seasonal
164 streamflow.

165 **2.3 Change Detection**

166 Three statistical methods were used to comprehensively examine the temporal changes in the
167 long-term hydro-climatic data series: (1) The Mann-Kendall test (Mann, 1945; Kendall, 1975) for
168 the non-linear trend at significance levels of $\alpha = 0.001, 0.01, 0.05,$ and $0.10,$ (2) The Sen's
169 nonparametric method was applied to examine the linear trend and to estimate the true slope of an
170 existing trend as change per year (Gilbert, 1987), and (3) The Dynamic Harmonic Regression
171 (DHR) method used for determining the change rates for meteorological, hydrological, and LAI
172 time series based on the Captain Toolbox (Taylor et al., 2007). The DHR model was used to fit
173 three main components in a time series including the trend of the original time series, the
174 periodicity, and the residuals, which were referred as Gaussian white noise for convenience. The
175 key feature of the DHR model is its ability to characterize the seasonal or periodic components of

176 time series data, so the method is suitable for analyzing time series with remarkable seasonal
177 variations. The DHR model analyzes the seasonal or periodic component using a similar approach
178 as Fourier analysis.

179 We used a series of common hydrologic detection methods to determine magnitude and
180 timing of the effects of land use change and climate change on streamflow (Ma et al., 2010; Tang
181 et al., 2011; Wei and Zhang, 2012). The Flow Duration Curve (FDC) (Vogel and Fennessey, 1993)
182 and the Double Mass Curve (DMC) methods (Wei and Zhang, 2010) were used to determine
183 changes of streamflow frequency in daily and annual streamflow as a result of urbanization,
184 respectively.

185 The trend of the baseflow component of the streamflow is one important indicator of change
186 in soil water storage, i.e., soil moisture and groundwater conditions (Price et al., 2011). The
187 Baseflow Index (BFI) program was used to separate the baseflow from measured total daily
188 streamflow (Wahl and Wahl, 1995). Our results showed that N , the number of days over which a
189 minimum flow could be determined, was 7 days for the study basin (Figure 5), suggesting that BFI
190 (baseflow/streamflow ratio) would not change much shorter than 7 days. We used a value of 0.9
191 for the turning point factor (f) to remove daily streamflow greater than $100 \text{ m}^3 \text{ s}^{-1}$. Details of the
192 methods to determine N and f can be found in Wahl and Wahl (1995).

193 **2.4 Attribution Analysis**

194 Once hydrologic change point was detected, we determined the individual contributions of climate
195 and landcover/land use change to the observed streamflow change. We assumed that that the
196 observed streamflow change (ΔQ) in the study basin could be explained by the sum of change in

197 climate (ΔQ_{clim}) and change in land use/land cover (i.e., urbanization) (ΔQ_{lulc}):

198
$$\Delta Q = \Delta Q_{clim} + \Delta Q_{lulc}$$

199 Then, the contribution of landcover/landuse ($\% \Delta Q$) can be estimated as:

200
$$\% \Delta Q_{lulc} = (\Delta Q - \Delta Q_{clim}) / \Delta Q * 100, \text{ or}$$

201
$$\% \Delta Q_{lulc} = (1 - \Delta Q_{clim} / \Delta Q) * 100$$

202 ΔQ = observed mean annual Q in the second period – Q in reference period (i.e., \bar{Q}_0)

203 We used the Climate Elasticity Model (CEM) and the Rainfall-Runoff model (RRM) to determine
204 ΔQ_{clim} (Li et al., 2007). The CEM involved developing an empirical relationship between deviation
205 of Q (ΔQ_{0i}) and deviations P (ΔP_{0i}) and PET (ΔPET_{0i}) from the long-term means for the
206 reference period:

$$\frac{\Delta Q_{0i}}{\bar{Q}_0} = \alpha \cdot \frac{\Delta P_{0i}}{\bar{P}_0} + \beta \cdot \frac{\Delta PET_{0i}}{\bar{PET}_0}$$

207 Where, α and β were fitted ‘climate sensitivity’ parameters derived from annual climate data for
208 the reference period (1986-2002) in this study as determined by the double mass method) while
209 \bar{Q}_0 and \bar{P}_0 were mean measured annual streamflow and precipitation. \bar{PET}_0 represents mean
210 annual potential ET estimated by the FAO reference ET method (Allen et al., 1994). Then, the
211 effects of the climate change in the second period in question could be calculated as:

$$\Delta \bar{Q}_{clim} = \bar{Q}_{pre} - \bar{Q}_0$$

212 Where $\Delta \bar{Q}_{clim}$, \bar{Q}_{pre} , \bar{Q}_0 represents the mean effects of climate change on annual streamflow
213 during the second period, predicted mean streamflow using the climate (P and PET) for the second
214 period and the empirical equation developed from the reference period, and observed streamflow

215 during the reference period, respectively.

216 The second model Rainfall-Runoff Model (RRM) was chosen to strengthen the attribution
217 analysis by considering the seasonal climatic variability. This method involved developing the
218 relationships between Q, P, and the variances (σ_{oi}^2) of P calculated using monthly P data series
219 without consideration of PET (Jones et al, 2006; Li et al., 2007):

$$Q_{oi} = a + bP_{oi}(\sigma_{oi}^2)^c$$

220 Where Q_{oi} and P_{oi} is the annual Q and P for the reference period, respectively while σ_1^2 is the
221 variance of the monthly P. The values of the three parameter, a , b , and c were derived using data
222 from the reference period. The empirical model was then applied to estimate annual streamflow
223 using precipitation for the second period (Q_{pre}) and finally to calculate the mean changes in Q
224 ($\Delta\bar{Q}_{clim}$) as the differences between \bar{Q}_{pre} and mean streamflow for the reference period (\bar{Q}_0).

225 **3 Results**

226 **3.1 Land conversion and change in LAI**

227 During 2000-2012, the QRB has gone through dramatic land cover changes characterized by an
228 increase in urban areas and a decrease in paddy fields (Du et al., 2011, 2012; Chen and Du, 2014)
229 (see insert in Figure 2). The land cover change matrix showed that, from 2000 to 2012, the area of
230 urban built-up areas increased 388 km² or 174% at the expense of dry crop lands (decreased 43
231 km², or 6%), paddy fields (decreased 255 km², or 21%), and forest lands (decreased 83 km², or
232 23%) (Table 1). Since dryland changed relatively small from 2000 to 2012 (insert Figure 2 and
233 Table 1), majority of detected reduction in cropland area came from the changes in paddy fields.

234 MODIS data indicated that both mean annual and peak growing season watershed level LAI

235 decreased significantly ($p < 0.05$) with Z statistic = -2.08 and Z statistic = -2.41, respectively
236 (Table 2) (Figure 6). Since the major decrease in land use was paddy rice, the decline of LAI was
237 mainly caused by land conversion of paddy field to urban uses. The decrease trend of LAI
238 followed a similar pattern as ET during 2000-2013.

239 **3.2 Trend in Climate and MODIS ET**

240 The M-K test showed that the growing season precipitation had a weak increasing trend, but
241 annual total precipitation had an insignificant decreasing trend during 2000-2013 (Table 2). The
242 mean annual air temperature showed an insignificant change, but with an weak increase of 0.07°C
243 yr^{-1} in the peak growing season from July to August (Table 2). Both annual and growing season
244 PET rose significantly by 7.5 mm yr^{-1} (Z statistic = 2.5, $p < 0.05$) and 5.1 mm yr^{-1} (Z statistic =
245 2.4, $p < 0.05$), respectively, an opposite trend of the actual ET (Table 2). The DHR method also
246 identified a rising trend for annual PET.

247 The mean annual MODIS ET was 655 mm yr^{-1} , varying from a low of 598 mm yr^{-1} in 2011
248 to the highest 715 mm yr^{-1} in 2002 during the study period (2000-2013). Annual ET exhibited a
249 general decreasing trend (-3.6 mm yr^{-1}) and pronounced decreases in the peak growing season of
250 July to August (-1.7 mm yr^{-1} , Z statistic = -2.3, $p < 0.05$) (Table 2) (Figure 4). The ET linear trend
251 during the peak growing season (July-August) accounted for 32% of the total annual trend. Overall,
252 ET showed a similar decreasing trend with LAI in the peak growing season during 2000-2013
253 (Figure 6). Annual ET and the peak growing season ET departures from the long-term means had
254 significantly positive correlations with LAI departures ($R = 0.46$, $p = 0.1$; $R = 0.64$, $p = 0.015$,
255 respectively), but weak negative correlations with PET departures ($R = -0.38$, $p = 0.18$) (Figure 7).

256 **3.3 Changes in streamflow characteristics**

257 The FDC analysis for the flow measured at Wuding Sluice Gate indicated that both daily
258 highflows and lowflows were elevated during 2009-2013 compared to 2002-2008, with the median
259 flow rates increased from $30\text{m}^3\text{s}^{-1}$ to $38\text{m}^3\text{s}^{-1}$ (Figure 8). The extreme high flow in 2002-2008 was
260 caused by one extreme rainfall event in July, 2007 (rainfall = 339 mm) that resulted in widespread
261 flooding. The baseflow analysis also showed a significant ($p = 0$) increasing trend during
262 2006-2013 (Figure 9). The increase in baseflow or low flow coincided with the observations that
263 the groundwater levels in the study basin were on the rise in recent decade as a result of
264 groundwater management and likely landuse change in the recent decade (Figure 10). The runoff
265 coefficient (Streamflow/Precipitation ratio) during May-October period (wet, flooding seasons)
266 increased significantly from 0.32 to 0.41, or 28%, during 2002-2013 (Z statistic = 2.89, $p < 0.01$)
267 (See insert in Figure 8).

268 **3.4 Changes in Annual Watershed Water Balances**

269 The DMC analysis identified a clear 'break point' of total annual streamflow (Q) around 2003
270 (Figure 11). The slopes of the regression lines between accumulated precipitation and streamflow
271 increased from 0.27 to 0.50. Mean annual streamflow significantly increased from 353 mm to 556
272 mm from period 1 (1986-2002) to period 2 (2003-2013) (Figure 12). This represented an increase
273 of runoff coefficient (Q/P) from 0.32 to 0.49, a 53% increase. The trend of annual streamflow was
274 influenced heavily by year 1991, a huge flooding event occurred in the Yangtze River Basin.
275 When this year was removed, R^2 increased from 0.1 to 0.34 and p value increased to a highly
276 significant level ($p = 0.002$). In the meantime, annual ET as estimated by P-Q, decreased
277 significantly from 752 mm to 578 mm from period 1 to period 2, representing a decline in ET by

278 23% or ET/P ratio by 25%.

279

280 3.5. Contributions of landuse/landcover change (LULC) ($\% \Delta Q_{lulc}$) and climate change and
281 variability ($\% \Delta Q_{clim}$)

282 The two models gave rather similar results on the contributions of climate change and LULC
283 to the observed change in streamflow from the reference period of 1986-2002 to the evaluation
284 period 2003-2013 (Table 3). On average, the increase in precipitation contributed 13-18% of the
285 increased streamflow of 203 mm yr⁻¹ between the two periods while other factors, LULC in this
286 case, contributed 82-87% of the streamflow change. Within the contributions of climate (P and
287 PET), the CEM modeling analysis suggested that PET did not significantly influence streamflow
288 and thus was not used to explain the variability of streamflow change. Using P alone explained
289 about 90% of the observed variability of streamflow. In theory, the increase in PET could have
290 reduced streamflow due to the influence on ET.

291 **4 Discussion**

292 **4.1 Increased streamflow explained by the decreases in ET and LAI**

293 The total streamflow (Figure 12, Table 3), highflows, and lowflows (Figures 8, 9) in the QRB
294 have substantially increased during 2000-2013 while both LAI and ET have decreased (Figure 6,
295 Figure 12). Based on the watershed balance theory and comprehensive analyses using different
296 method including FDC, CEM, RRM, we attributed the dramatic increase in streamflow mainly to
297 the changes in LULC and associated decrease in LAI, not climate (PET or P), for the following
298 three complementary reasons.

299 First, LAI is a major controlling factor for ET, especially during the growing season (Sun et al.,
300 2011a, 2011b; Sun and Lockaby, 2012) and in humid, energy-limited southern China in particular
301 (Liu et al., 2013). The strong relationship between MODIS ET and LAI (Figures 6, Figure 7)
302 supported our hypothesis that urbanization dramatically reduced ET due to the reduction of LAI,
303 thus explained the observed increase in streamflow.

304 Second, regional annual ET is generally controlled by PET, P, and land surface conditions (Sun
305 et al., 2005). A decrease in ET is normally caused by a decrease in P and/or PET (Sun et al., 2005;
306 Sun et al., 2011a, 2011b). Our data suggested that the decrease in ET was not caused by PET or P
307 because annual and growing season PET significantly increased and overall precipitation did not
308 change significantly. In fact, a negative correlation was found between ET and PET departures
309 (Figure 7). The DMC method that eliminated precipitation effects on streamflow suggested the
310 QRB had a shift of annual streamflow upward around 2003 (Figure 11). The two models for
311 climate attribution analysis converged indicating that LULC contributed about 85% of the observed
312 variability in streamflow and precipitation contributed about 15%. PET increased more
313 dramatically during 2003-2013 than during 1986-2002 (Figure 12). The increase in PET might
314 have masked the decrease of ET due to change in LULC, so we argue that the estimated 85%
315 contribution from LULC is a conservative estimate.

316 Third, the large decrease in LAI as detected by remote sensing corresponded closely to the
317 dramatic conversion of rice paddy fields and increase in total impervious area (TIA) during the
318 urbanization campaign in the QRB since the early 2000s. Previous studies in the United States
319 suggest that stream flow and water quality regimes are degraded when the TIA exceeds 10-20% of
320 total watershed area (Arnold and Gibbons, 1996; Bledsoe and Watson, 2001). Our study result was

321 consistent with the finding of the threshold response in the literature, perhaps in the lower end of
322 the spectrum (<10%). The detected decrease in LAI due to shrinking rice paddy areas has
323 overwhelmed the impacts of climate change (i.e. rise of PET) on ET, highlighting the importance
324 of LULC change in evaluating environmental change in the study region.

325 **4.2 Regional hydrologic and environmental implications**

326 Our findings complement findings from an earlier study for the same basin. Du et al. (2011, 2012)
327 conducted a simulation study suggesting that the elevated highflows were mostly due to an
328 increase in impervious surface area. Our new analysis suggested that in addition to the increase in
329 impervious surface areas other factors such as reduced ET could be the main causes that
330 contributed to the observed increase in total flow and baseflows in the study basin. The present
331 study advanced the understanding of the processes of hydrologic disturbances. Study results had
332 important hydrological and environmental implications for paddy field-dominated regions in
333 China and elsewhere in East Asia.

334 First, we confirmed our hypothesis that converting water stress- free paddy fields to relatively
335 'dry' urban uses or impervious surfaces dramatically reduced ET (Figure 1). Thus, converting
336 wetlands, such as paddy fields, to impervious or built-up areas is expected to have a much higher
337 magnitude of hydrologic impacts than that for converting dry croplands or forests to urban land
338 uses. The ET estimates based on two independent methods, watershed water balance and remote
339 sensing, all showed large decreases in ET.

340 Second, the populated study region is prone to floods and droughts due to the nature of a
341 strong summer monsoon climate (Gu et al., 2011). Urbanization is likely to exacerbate the flood
342 risks during the monsoon season as a result of decreased ET, an increased impervious surface area,

343 and decreased retention capacity of rice paddy fields (Kang et al., 1998; Kim et al., 2014). In
344 addition, an increase in stormflow has important concerns on stream channel stability, soil erosion,
345 and reactivation of streambed sediment and pollutants (Sun and Locakby, 2012). This is of
346 particular concern given the increasing trend of typhoon activities in southern China under climate
347 change (Gu et al., 2011).

348 Third, the increasing trend in baseflow found in this study is in somewhat contradiction to the
349 popular literature that suggests otherwise (Ott and Uhlenbrook, 2004; Kim et al., 2005; Price et al.,
350 2011). We argue that the large reduction in ET from paddy fields might have overwhelmed the
351 reduction of groundwater recharge from the increased impervious surfaces. The QRB is still
352 dominated by croplands (62% of land area in 2012) and the dramatic reduction in water loss from
353 rice cultivation and irrigation needs likely elevated groundwater recharge from uplands or stream
354 channels overall (Figure 10). Other studies have shown that reductions in forest land coverage,
355 thus reduction in ET, could increase baseflow in the humid piedmont region in North Carolina
356 (Boggs and Sun, 2011) and northeastern U.S. (Lull and Sopper, 1969). Boggs and Sun (2011)
357 conclude that the effects of vegetation removal on streamflow are most pronounced during the
358 growing seasons when the contrast between ET from a vegetated surface and from an urbanized
359 surface is the highest. Therefore, it is plausible that replacing paddy fields with high ET with urban
360 land uses (e.g., lawns or impermeable surfaces) with low ET may result in similar effect as forest
361 removal during urbanization. Future studies should examine the seasonality of the trend of
362 baseflow change to confirm the effects of rice paddy conversion on baseflow and groundwater
363 change.

364 Fourth, according to the regional energy balance theory, a strong reduction in ET or latent heat

365 from urbanization likely results in an increase in sensible heat (Dow and DeWalle, 2000), a major
366 energy source of ‘urban heat islands’ (UHI) effects. The QRB is known to be one of the ‘Four
367 Ovens’ in China for its hot summer weather and the area has seen a warming trend during the past
368 three decades (Figure 3). Although it is beyond the scope of this study to link the observed rising
369 air temperature and urban UHI to land use change in the study region, our study suggests that a
370 reduction in ET from paddy fields is likely to further aggravate the UHI effects under a humid
371 climate (Zhao et al., 2014). Our study is consistent with the notion by local people that paddy
372 fields behave as a large ‘air conditioner’. An earlier study indeed rated the region in the lower
373 Yangtze River Delta as the most impacted region from urbanization across China in terms of UHI
374 effects (He et al., 2007). A study on China’s 32 cities by Zhou et al. (2014) concluded that UHI
375 effects dropped more sharply from urban centers to the rural areas in the humid southern China
376 than in northern China or inland cities, indicating the stronger contrast of energy regime in the
377 paddy-dominated regions than in other regions. Our study offered new evidence to explain the
378 causes of the regional urban heat island effects from the point of view of ET and hydrological
379 process changes.

380 **5 Conclusions**

381 Using long term hydrometeorological records, land cover/land use change information, and remote
382 sensing-based biophysical and evapotranspiration data, this case study showed that streamflow
383 rates, both highflows and lowflows, in the Qinhuai River Basin have increased from 1986 to 2013.
384 A significant increase in streamflow and a decrease in ET in the study basin were detected, and the
385 changes were considered to be associated with urbanization characterized as shrinkage of rice

386 paddy fields and an increase in impervious surface area. Urbanization that resulted in a reduction
387 in LAI during the peak growing season overwhelmed the hydrological effects of climate warming
388 and precipitation variability during the study period. The importance of rice paddy fields in
389 regulating ET and hydrologic responses to disturbance has been underestimated in previous
390 similar studies. There is a research need to fully understand the ecohydrological processes that
391 control the effects of land conversions on land surface energy and water balances at multiple scales.
392 Models for assessing the ecosystem service function (e.g., climate cooling, flood retention) of rice
393 paddy fields must include proper algorithms describing the hydrological processes including ET
394 that links water and energy balances.

395 Rice cultivations have been practiced for thousands of years around the world. However,
396 converting rice paddy fields to other uses in southern China and East Asia has been on the rise
397 under a changing climate and demographics. Our study indicates that urbanization will likely
398 increase the risk of flooding, heat islands, and social vulnerability due to the loss of ecosystem
399 services of rice paddies. To minimize and mitigate the hydrologic and environmental impacts of
400 converting paddy fields down streams while maintaining resource sustainability requires an
401 integrated watershed management approach that involves careful urban planning (Dunne and
402 Leopold, 1978), landscape design (Dietz and Clausen, 2008), and irrigation management (Park et
403 al., 2009).

404

405 *Acknowledgements.* This study was supported by the Natural Science Foundation of China
406 (71373130), the Jiangsu Key Laboratory of Agricultural Meteorology Fund (No. KYQ1201), the
407 National Key Basic Research Program of China (2013CB430200, 2013CB430206), and IceMe of
408 NUIST. Partial support was from the Southern Research Station, USDA Forest Service.

409

410

411
412

413 **References**

- 414 Allen, R.G., Smith, M., Perrier, A., and Pereira, L. S.: An update for the definition of reference evapotranspiration,
415 ICID Bull., 43, 1-34, 1994.
- 416 Arnold, C.L., and Gibbons, C.J.: Impervious surface coverage: the emergence of a key environmental indicator, Am.
417 Planners Assoc. J., 62, 243-58, 1996.
- 418 Barron, O. V., Barr, A. D., and Donn, M. J.: Effect of urbanisation on the water balance of a catchment with shallow
419 groundwater, J. Hydrol., 485, 162-176, doi:10.1016/j.jhydrol.2012.04.027, 2013.
- 420 Bledsoe, B. P. and Watson, C. C.: Effects of urbanization on channel instability, J. Am. Water Resour. As., 37,
421 255-270, doi:10.1111/j.1752-1688.2001.tb00966.x, 2001.
- 422 Boggs, J. L. and Sun, G.: Urbanization alters watershed hydrology in the Piedmont of North Carolina, Ecohydrology,
423 4, 256-264, doi:10.1002/Eco.198, 2011.
- 424 Brath, A., Montanari, A., and Moretti, G.: Assessing the effect on flood frequency of land use change via hydrological
425 simulation (with uncertainty), J. Hydrol., 324, 141-153, doi:10.1016/j.jhydrol.2005.10.001, 2006.
- 426 Caldwell, P. V., Sun, G., McNulty, S. G., Cohen, E. C., and Myers, J. A. M.: Impacts of impervious cover, water
427 withdrawals, and climate change on river flows in the conterminous US, Hydrol. Earth Syst. Sc., 16,
428 2839-2857, doi: 10.5194/hess-16-2839-2012, 2012.
- 429 Chen, A. L., Du, J. K.: Simulation and forecast of land cover pattern in Qinhuai River Basin based on the CA- Markov
430 model, Remote Sensing for Land and Resources, 26(2): 184-189, doi:10.6046/gtzyyg.2014.02.29, 2014.
- 431 Dietz, M. E. and Clausen, J. C.: Stormwater runoff and export changes with development in a traditional and low
432 impact subdivision, J. Environ. Manage., 87, 560-566, doi:10.1016/j.jenvman.2007.03.026, 2008.
- 433 Du, J. K., Li, C., Rui, H., Li, Q., Zheng, D., Xu, Y. and Hu, S.: The change detection of impervious surface and its
434 impact on runoff in the Qinhuai River Basin, China, In: 19th International Conference on Geoinformatics IEEE
435 pp1-5, 2011.
- 436 Du, J. K., Qian, L., Rui, H. Y., Zuo, T. H., Zheng, D. P., Xu, Y. P., and Xu, C. Y.: Assessing the effects of urbanization
437 on annual runoff and flood events using an integrated hydrological modeling system for Qinhuai River basin,
438 China, J. Hydrol., 464, 127-139, doi:10.1016/j.jhydrol.2012.06.057, 2012.
- 439 Dunne, T. and Leopold, L.: Water in environmental planning (New York: W H Freeman and Company press), 1978.
- 440 Dow, C. L. and DeWalle, D. R.: Trends in evaporation and Bowen ratio on urbanizing watersheds in eastern United
441 States, Water Resour. Res., 36, 1835-1843, doi:10.1029/2000wr900062, 2000.
- 442 Foley, J. A., DeFries, R., Asner, G. P., Barford, C., Bonan, G., Carpenter, S. R., Chapin, F. S., Coe, M. T., Daily, G. C.,
443 Gibbs, H. K., Helkowski, J. H., Holloway, T., Howard, E. A., Kucharik, C. J., Monfreda, C., Patz, J. A.,
444 Prentice, I. C., Ramankutty, N., and Snyder, P. K.: Global consequences of land use, Science, 309, 570-574, doi:
445 10.1126/science.1111772, 2005.
- 446 Gilbert, R. O.: Statistical methods for environmental pollution monitoring (New York: VanNostrand Reinhold press),
447 1987.
- 448 Gong, P., Wang, J., Yu, L., Zhao, Y.C., Zhao, Y.Y., Liang, L., Niu, Z.G., Huang, X.M., Fu, H.H., Liu, S., Li, C.C., Li,
449 X.Y., Fu, W., Liu, C.X., Xu, Y., Wang, X.Y., Cheng, Q., Hu, L.Y., Yao, W.B., Zhang, H., Zhu, P., Zhao, Z.Y.,
450 Zhang, H.Y., Zheng, Y.M., Ji, L.Y., Zhang, Y.W., Chen, H., Yan, A., Guo, J.H., Yu, L., Wang, L., Liu, X.J., Shi,
451 T.T., Zhu, M.H., Chen, Y.L., Yang, G.W., Tang, P., Xu, B., Ciri, C., Clinton, N., Zhu, Z.L., Chen, J., and Chen, J.:
452 Finer resolution observation and monitoring of global land cover: first mapping results with Landsat TM and
453 ETM+ data, Int. J. Remote Sens., 34, 2607-2654, 2013.

454 Gu, C., Hu, L., Zhang, X., Wang, X., and Guo, J.: Climate change and urbanization in the Yangtze River Delta, *Habitat*
455 *Int.*,35,544-552, 2011.

456 He, B., Wang, Y., Takase, K., Mouri, G., and Razafindrabe, B. H. N.: Estimating Land Use Impacts on Regional Scale
457 Urban Water Balance and Groundwater Recharge, *Water Resour.Manag.*, 23, 1863-1873,doi:
458 10.1007/s11269-008-9357-2, 2009.

459 He, J. F., Liu, J. Y., Zhuang, D. F., Zhang, W., and Liu, M. L.: Assessing the effect of land use/land cover change on
460 the change of urban heat island intensity, *Theor. Appl. Climatol.*, 90, 217-226,doi:10.1007/s00704-006-0273-1,
461 2007.

462 Jacobson, C. R.: Identification and quantification of the hydrological impacts of imperviousness in urban catchments:
463 A review, *J. Environ.Manage.*, 92, 1438-1448, 2011.

464 Jones, R.N., Chiew, F.H.S., Boughton, W.C., and Zhang, L.: Estimating the sensitivity of mean annual runoff to
465 climate change using selected hydrological models. *Adv. Water Resour.*, 29, 1419-1429, doi:
466 10.1016/j.advwatres.2005.11.001, 2006.

467 Jonsson, P. and Eklundh, L.: TIMESAT - a program for analyzing time-series of satellite sensor data, *Comput.*
468 *Geosci-Uk*, 30, 833-845, 2004.

469 Kang, I. S., Park, J. I., and Singh, V. P.: Effect of urbanization on runoff characteristics of the On-Cheon stream
470 watershed in Pusan, Korea, *Hydrol. Process*, 12, 351-363, 1998.

471 Kendall, M. G.: Rank correlation methods London: Charles Griffin press, 1975.

472 Kim, S. J., Kwon, H. J., Park, G. A., and Lee, M. S.: Assessment of land-use impact on streamflow via a grid-based
473 modelling approach including paddy fields, *Hydrol. Process.*, 19, 3801-3817,doi:10.1002/Hyp.5982, 2005.

474 Kim, Y. J., Kim, H. D., and Jeon, J. H.: Characteristics of Water Budget Components in Paddy Rice Field under the
475 Asian Monsoon Climate: Application of HSPF-Paddy Model, *Water-Sui.*, 6, 2041-2055,
476 doi:10.3390/W6072041, 2014.

477 Li L-J, Zhang, L, Wang, H, Wang, J, Yang, J-W, Jiang, D-J, Li, J-Y, and Qin, D-Y.: Assessing the impact of climate
478 variability and human activities on streamflow from the Wuding River basin in China, *Hydrol. Process.*, 21,
479 3485-3491, doi: 10.1002/hyp.6485, 2007.

480 Liu, Y., Zhou, Y., Ju, W., Chen, J., Wang, S., He, H., Wang, H., Guan, D., Zhao, F., Li, Y., and Hao, Y.:
481 Evapotranspiration and water yield over China's landmass from 2000 to 2010, *Hydrol. Earth Syst. Sci.*, 17,
482 4957-4980, doi:10.5194/hess-17-4957-2013, 2013.

483 Lull, H.W. and Sopper, W.E.: Hydrologic effects from urbanization of forested watersheds in the Northeast. USDA
484 Forest Service Research Paper NE-146.Northeastern Forest Experiment Station, 1969.

485 Ma, H. A., Yang, D. W., Tan, S. K., Gao, B., and Hu, Q. F.: Impact of climate variability and human activity on
486 streamflow decrease in the Miyun Reservoir catchment, *J. Hydrol.*, 389,
487 317-324,doi:10.1016/j.jhydrol.2010.06.010, 2010.

488 Mann, H. B.: Non-parametric test against trend, *Econometrica*, 13, 245-259, 1945.

489 McDonald, R. I., Green, P., Balk, D., Fekete, B. M., Revenga, C., Todd, M., and Montgomery, M.: Urban growth,
490 climate change, and freshwater availability, *P. Natl. Acad. Sci. USA*, 108, 6312-6317,doi:
491 10.1073/pnas.1011615108,2011.

492 Miller, J. D., Kim, H., Kjeldsen, T. R., Packman, J., Grebby, S., and Dearden, R.: Assessing the impact of urbanization
493 on storm runoff in a pen-urban catchment using historical change in impervious cover, *J. Hydrol.*, 515,
494 59-70,doi:10.1016/j.jhydrol.2014.04.011, 2014.

495 Mu, Q. Z., Zhao, M. S., and Running, S. W.: Improvements to a MODIS global terrestrial evapotranspiration
496 algorithm, *Remote Sens. Environ.*, 115, 1781-1800,doi: 10.1016/j.rse.2011.02.019, 2011.

497 Ott, B. and Uhlenbrook, S.: Quantifying the impact of land-use changes at the event and seasonal time scale using a

498 process-oriented catchment model, *Hydrol. Earth Syst. Sc.*, 8, 62-78, 2004.

499 Paul, M. J. and Meyer, J. L.: Streams in the urban landscape, *Annu. Rev. Ecol. Syst.*, 32, 333-365, 2001.

500 Price, K., Jackson, C. R., Parker, A. J., Reitan, T., Dowd, J., and Cyterski, M.: Effects of watershed land use and
501 geomorphology on stream low flows during severe drought conditions in the southern Blue Ridge Mountains,
502 Georgia and North Carolina, United States, *Water Resour. Res.*, 47,W02516,doi:10.1029/2010wr009340, 2011.

503 Roderick, M. L., Hobbins, M. T., and Farquhar, G. D.: Pan evaporation trends and the terrestrial water balance. II.
504 Energy balance and interpretation, *Geogr. Compass*, 3, 761-780, 2009.

505 Sakaguchi, A., Eguchi, S., and Kasuya, M.: Examination of the water balance of irrigated paddy fields in SWAT 2009
506 using the curve number procedure and the pothole module, *Soil Sci. Plant Nutr.*, 60,
507 551-564,doi:10.1080/00380768.2014.919834,2014.

508 Sun, G., McNulty, S. G., Lu, J., Amatya, D. M., Liang, Y., and Kolka, R. K.: Regional annual water yield from forest
509 lands and its response to potential deforestation across the southeastern United States, *J. Hydrol.*, 308,
510 258-268,doi: 10.1016/j.jhydrol.2004.11.021,2005.

511 Sun, G., Alstad, K., Chen, J. Q., Chen, S. P., Ford, C. R., Lin, G. H., Liu, C. F., Lu, N., McNulty, S. G., Miao, H. X.,
512 Noormets, A., Vose, J. M., Wilske, B., Zeppel, M., Zhang, Y., and Zhang, Z. Q.: A general predictive model for
513 estimating monthly ecosystem evapotranspiration, *Ecohydrology*, 4, 245-255,doi: 10.1002/Eco.194, 2011a.

514 Sun, G., Caldwell, P., Noormets, A., McNulty, S. G., Cohen, E., Myers, J. M., Domec, J. C., Treasure, E., Mu, Q. Z.,
515 Xiao, J. F., John, R., and Chen, J. Q.: Upscaling key ecosystem functions across the conterminous United
516 States by a water-centric ecosystem model, *J. Geophys. Res-Bioge.*, 116,doi:10.1029/2010jg001573, 2011b.

517 Sun, G. and Lockaby, B.G.: Chapter 3: Water quantity and quality at the urban-rural interface. In: D N Laband, B G
518 Lockaby and W Zipperer (Eds). *Urban-Rural Interfaces: Linking People and Nature*. (ASACSS, SSAmerica,
519 Madison, WI) pp26-45, 2012.

520 Tang, L. H., Yang, D. W., Hu, H. P., and Gao, B.: Detecting the effect of land-use change on streamflow, sediment and
521 nutrient losses by distributed hydrological simulation, *J. Hydrol.*, 409,
522 172-182,doi:10.1016/j.jhydrol.2011.08.015, 2011.

523 Taylor, C. J., Pedregal, D. J., Young, P. C., and Tych, W.: Environmental time series analysis and forecasting with the
524 Captain toolbox, *Environ. Modell. Softw.*, 22, 797-814,doi: 10.1016/j.envsoft.2006.03.002, 2007.

525 Tsai, M. H.: The Multi-functional roles of paddy field irrigation in Taiwan, *Proceedings of the pre-symposium for the*
526 *third world water forum (WWF3)*, 217-220, 2002.

527 Vogel, R. M. and Fennessey, N. M.: L-Moment Diagrams Should Replace Product Moment Diagrams, *Water Resour.*
528 *Res.*, 29, 1745-1752,1993.

529 Wahl, K. L. and Wahl, T. L.:Determining the flow of Comal Springs at New Braunfels, Texas, *Texas Water*
530 *'95*, American Society of Civil Engineers (San Antonio, Texas), pp77-86, August 16-17, 1995.

531 Wang, Y. J., Lv, H. J., Shi, Y. F., and Jiang, T.: Impacts of land use changes on hydrological processes in an
532 urbanized basin: a case study in the Qinhuai River Basin, *J. Nat. Resour.*, 24, 30-36, 2009.

533 Wei, X. H. and Zhang, M. F.: Quantifying streamflow change caused by forest disturbance at a large spatial scale: A
534 single watershed study, *Water Resour. Res.*, 46,W12525,doi: 10.1029/2010wr009250, 2010.

535 Wu, R.S., Sue, W.R.,and Chang, J.D.: A simulation model for investigating the effects of rice paddy fields on runoff
536 system In: Zenger A and Argent RM (eds) *MODSIM97 International Congress on Modelling and Simulation*.
537 *Modelling and Simulation Society of Australia and New Zealand*, pp 422-427, 1997.

538 Xiao, Y., An, K., Xie, G., and Lu, C.: Evaluation of Ecosystem Services Provided by 10 Typical Rice Paddies in
539 China, *J. Resour. Ecol.*, 2, 328-337, 2011.

540 Yuan, H., Dai, Y. J., Xiao, Z. Q., Ji, D. Y., and Shangguan, W.: Reprocessing the MODIS Leaf Area Index products for
541 land surface and climate modelling, *Remote Sens. Environ.*, 115, 1171-1187,doi: 10.1016/j.rse.2011.01.001,

542 2011.

543 Zhao, L., Lee, X., Smith, R. B., and Oleson, K.: Strong contributions of local background climate to urban heat islands,

544 Nature, 511, 216-219,doi: 10.1038/Nature13462, 2014.

545 Zhou, D, Zhao, S, Liu, S, Zhang, L, and Zhu C: Surface urban heat island in China's 32 major cities: Spatial patterns

546 and drivers. Remote Sens. Environ., 152, 51-61, 2014.

547

Table 1. The conversion matrix for land use change during 2000-2012 in the Qinhuai River Basin.

2000 (km ²)	2012 (km ²)					Σ (2000)
	Dry crop lands	Paddy fields	Forest	Water	Urban built-up areas	
Dry crop lands	320	226	7	8	175	736
Paddy fields	257	681	6	24	220	1,188
Forest	74	2	264	2	24	366
Water	16	12	2.36	59	14	104
Urban built-up areas	26	13	3	3	178	223
Σ (2012)	693	933	283	96	611	2,617
Area change from 2000 to 2012	-43	-255	-83	-8	388	--
Area change from 2000 to 2012 (%)	-6	-21	-23	-8	174	--

551 **Table 2.** Summary of Z statistics by the Nonparametric Mann-Kendall trend tests for temperature
 552 (T), ET, PET, precipitation (P), and LAI during the periods of July-August, April-October, and
 553 annual, Qinhuai River Basin (2000-2013).

Periods	Z statistic				
	LAI(s)	ET(s) (mm)	PET(s) (mm)	P(s) (mm)	T(s) (°C)
July-August	-2.41 [*] (-0.04)	-2.3 [*] (-1.7)	1.3(2.4)	1.31(12.9)	1.31(0.07)
April-October	-2.30 [*] (-0.02)	-1.2(-2.4)	2.4 [*] (5.1)	0.11(2.6)	0.77(0.02)
Annual	-2.08 [*] (-0.01)	-1.5(-3.6)	2.5 [*] (7.5)	-0.55(-8.0)	0.00(-0.00)

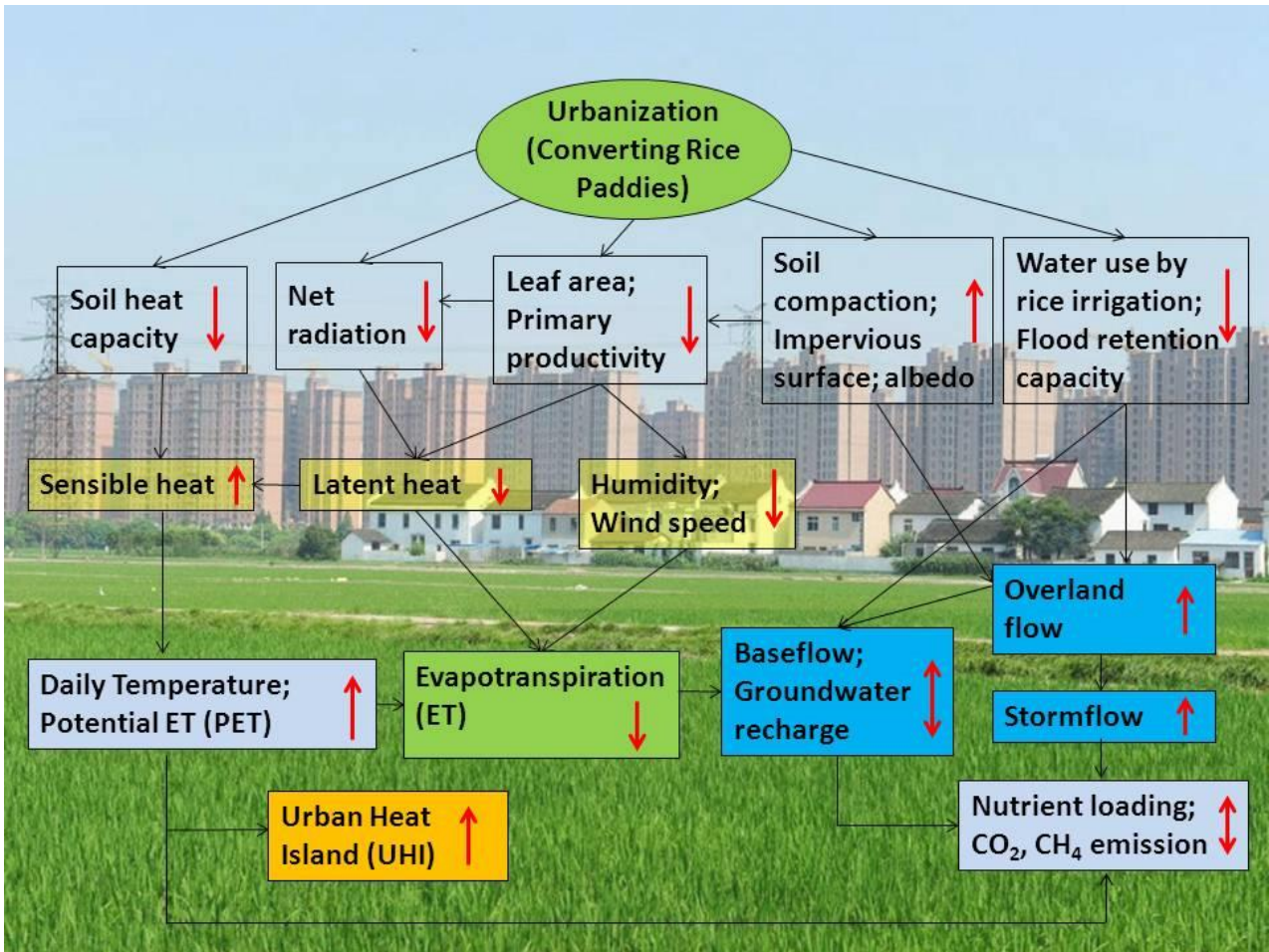
554 ^{*}Denotes significance level of 0.05. ‘s’ is the true slope of the linear trend, i.e., change per year.
 555

556 **Table 3.** Modeled contributions of land use change and climate change on the increase in
 557 streamflow (mm yr^{-1}) by the Climate Elasticity Model (CEM) and Rainfall Runoff Model (RRM).

Period	\bar{P}	\overline{PET}	\bar{Q}	ΔQ_o	CEM		RRM	
					$(\alpha=2.93; \beta=0.)$		$(a=-509; b=0.45; c=0.064)$	
					$\Delta\bar{Q}_{clim}$	$\Delta\bar{Q}_{lulc}$	$\Delta\bar{Q}_{clim}$	$\Delta\bar{Q}_{lulc}$
1986-2002 (reference)	1,105±291	998±82	353±287	--				
2003-2013	1,134±178	1,075±45	556±145	203	27 ± 166(13%)	177 ± 103(87%)	36 ± 169(18%)	167 ± 100(82%)

558
 559
 560
 561
 562
 563
 564
 565

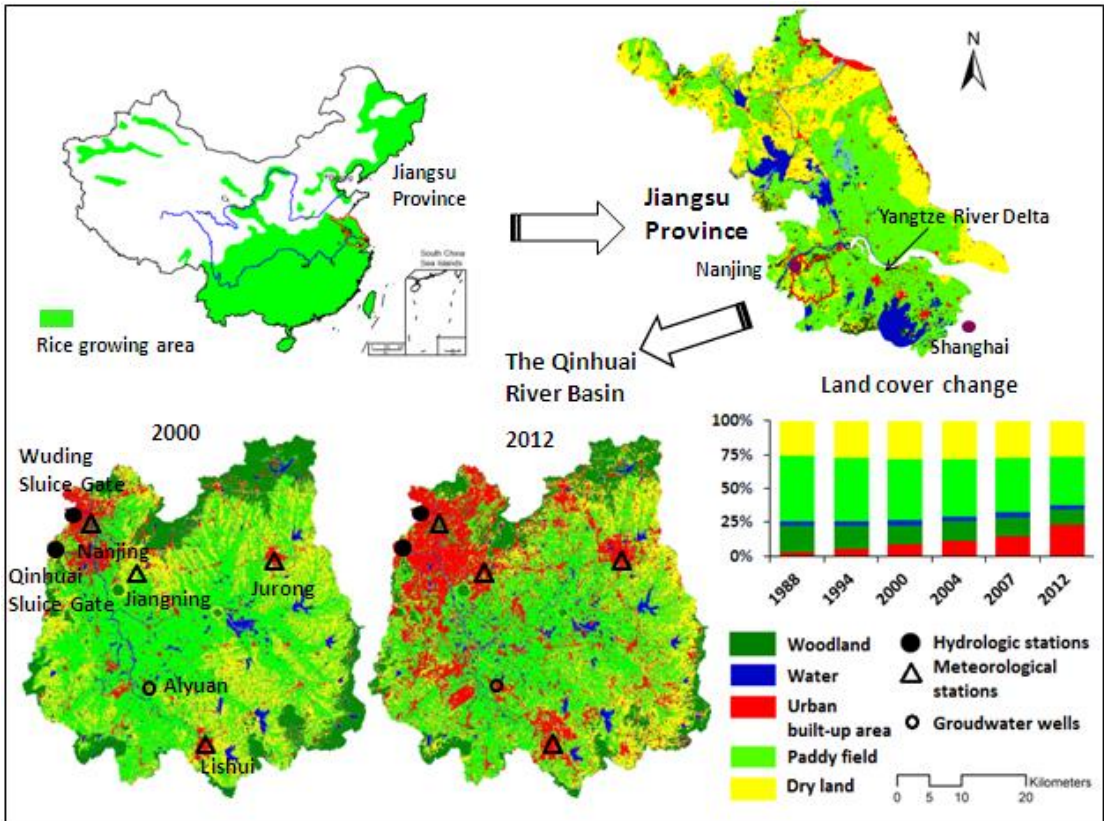
566
567



568
569

570 **Fig. 1.** A conceptual model illustrating the potential hydrologic and environmental impacts of
571 converting rice paddies to urban uses in the Yangtze River Delta region. Arrows represent
572 directions (up or down or both) of change (Background photo credit:
573 <http://blog.sciencenet.cn/blog-578415-712508.html>).

574
575
576



577

578 **Fig. 2.** Watershed location, instrumentation, and land use change patterns in the Qinhuai River
 579 Basin, Yangtze River Delta in southern China. The insert map showing changes in land use derived
 580 from published data (Du et al., 2012; Chen and Du, 2014) (1988 and 1994) and Landsat 7 ETM+
 581 images (2000-2012).

582

583

584

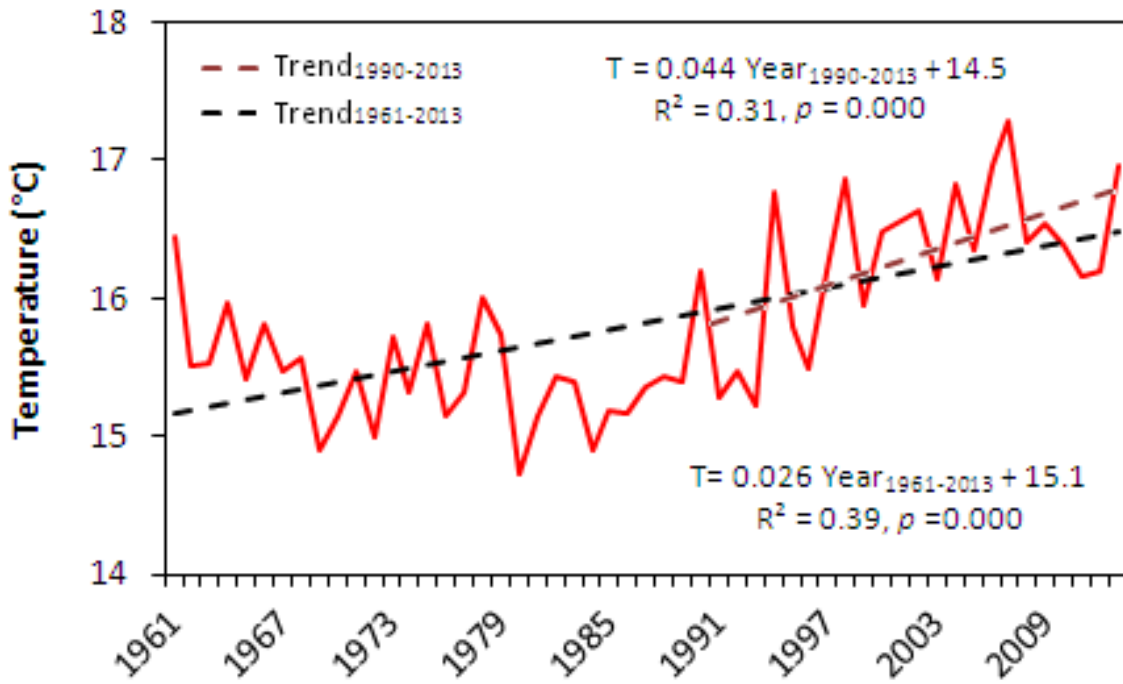
585

586

587

588

589



590

591 **Fig. 3.** Mean annual air temperature change across four meteorological stations in the Qinhuai

592 River Basin in southern China during 1961-2013.

593

594

595

596

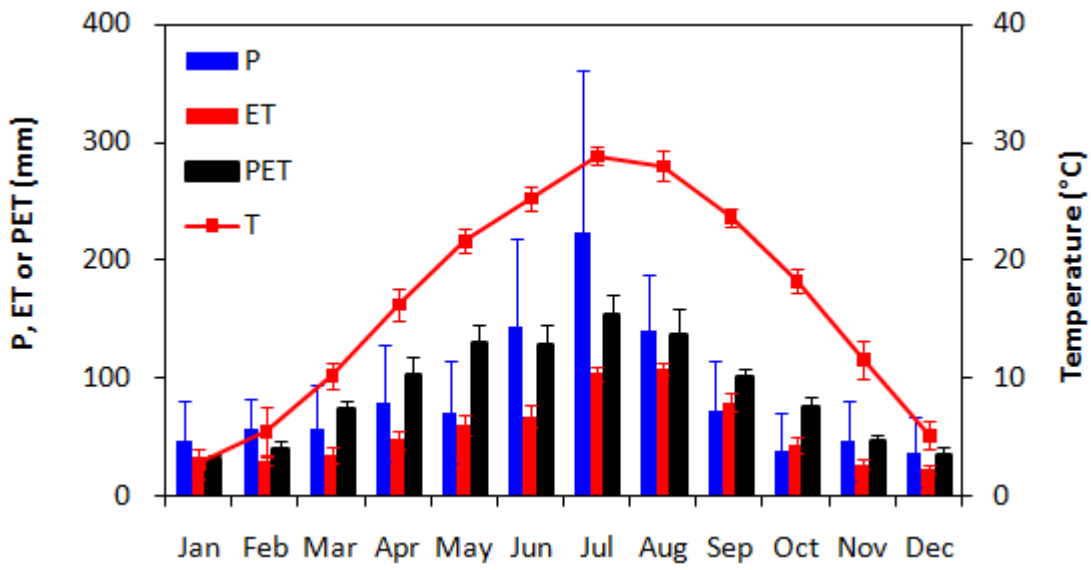
597

598

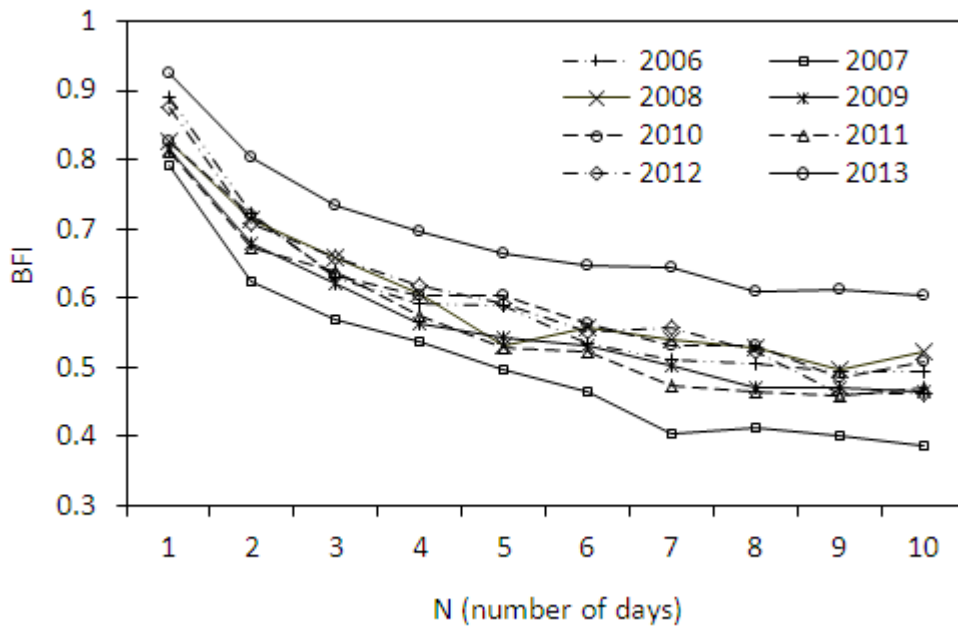
599

600

601



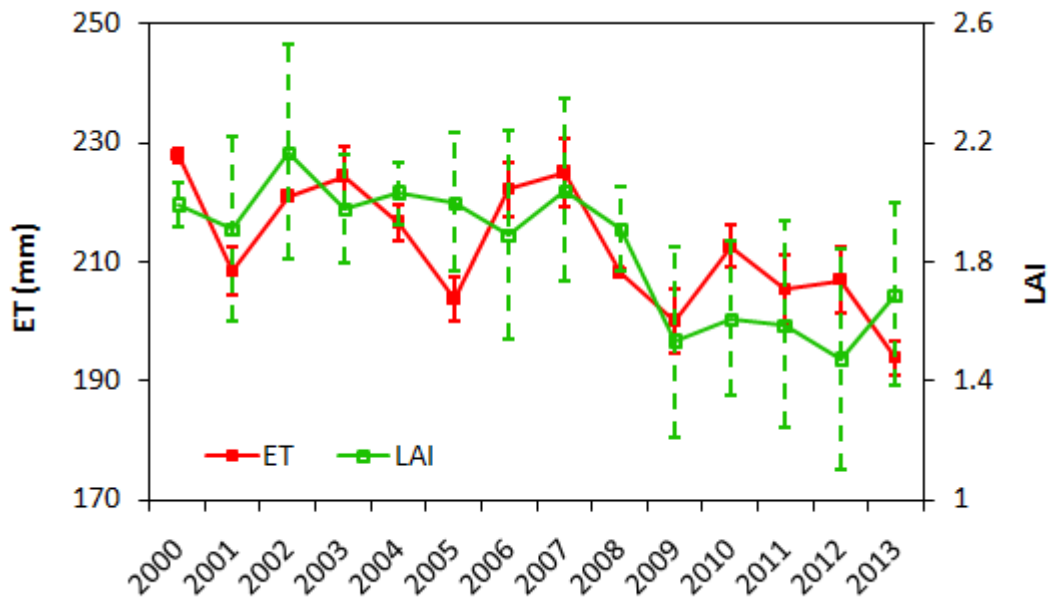
602 **Fig. 4.** Mean monthly precipitation (P), MODIS evapotranspiration (ET), potential
 603 evapotranspiration (PET) and temperature (T) (1986-2013), and the vertical lines are standard
 604 deviation.
 605



606

607 **Fig. 5.** Sensitivity of Base-flow Index (BFI) to the number of days (N) used to select the minimum
 608 value in baseflow separation analysis from 2006 to 2013 at the Wuding Station located at the
 609 outlet of the Qinhui River Basin.

610



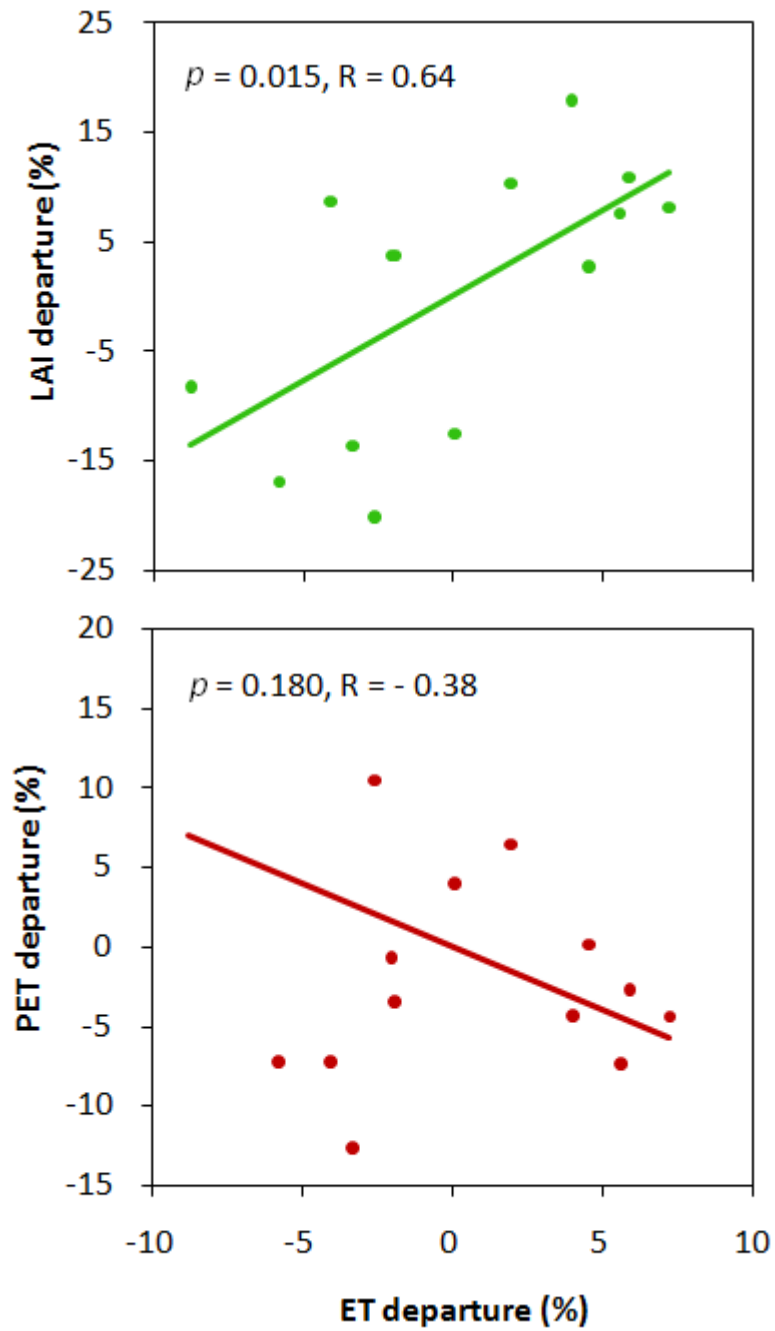
612

613 **Fig. 6.** Total MODIS ET (mm per two months) and mean LAI during the peak growing season

614 (July - August) over 2000-2013 in the Qinhuai River Basin. Vertical lines represent one standard

615 deviation across space.

616



617

618 **Fig. 7.**Correlations of the departures of basin-level ET with (a) the departures of mean leaf area

619 index (LAI) and (b) the departures of PET in the peak growing season (July-August) in the Qinhui

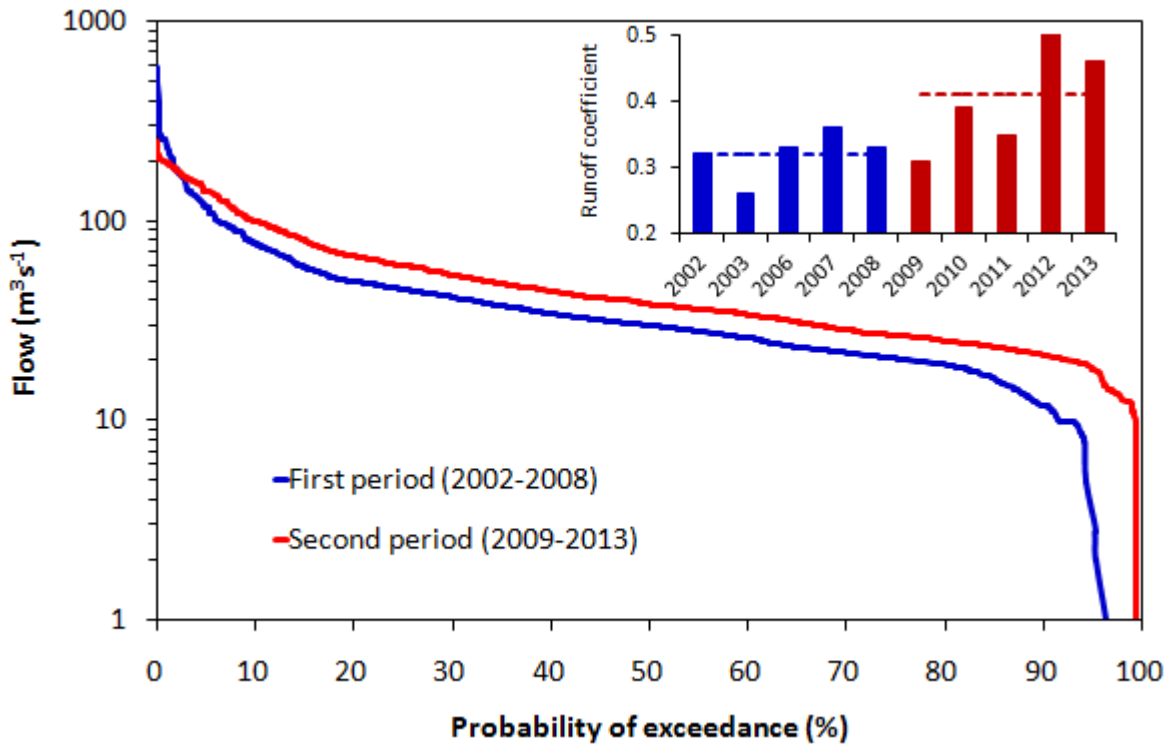
620 River Basin.

621

622

623

624



626

627 **Fig. 8.** Flow duration curves for mean daily flow in the first period (2002-2003 and 2006-2008)
 628 and the second period (2009-2013) (May-October) measured at the Wuding Station in the Qinhuai
 629 River Basin. Insert is runoff coefficient, the ratio of streamflow/precipitation for the period from
 630 May to October when the flow control gate was open.

631

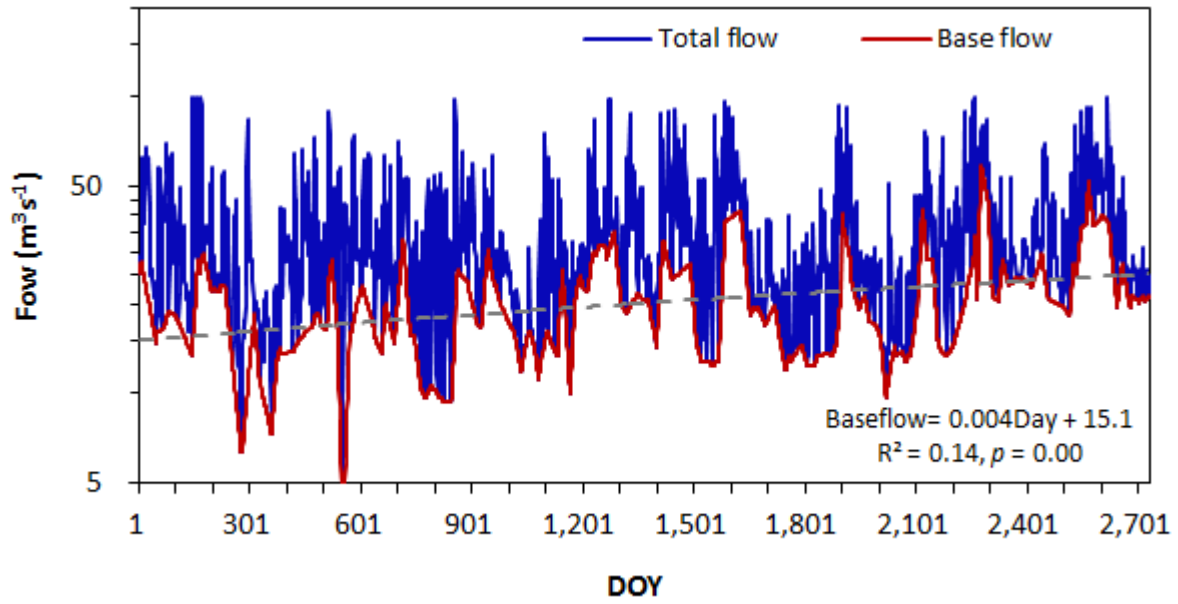
632

633

634

635

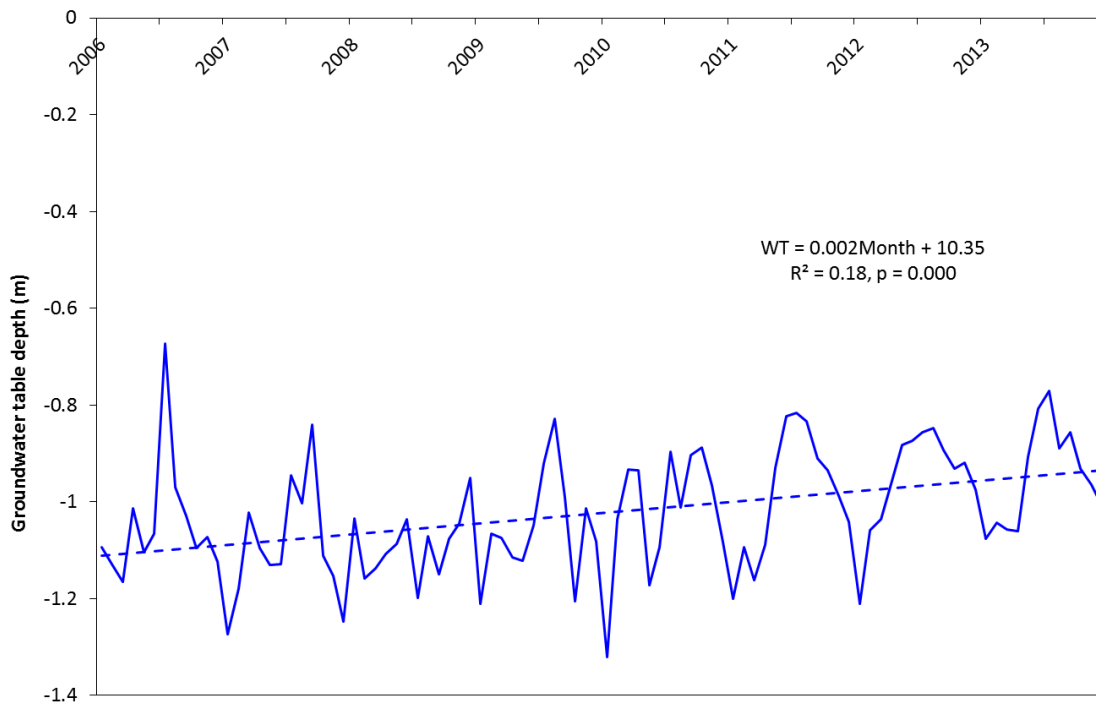
636



637

638 **Fig. 9.** Trend of daily base flow separated from total stream flow measured at the Wuding Station

639 during 2006-2013. DOY is the number of accumulated days since January 1, 2006.

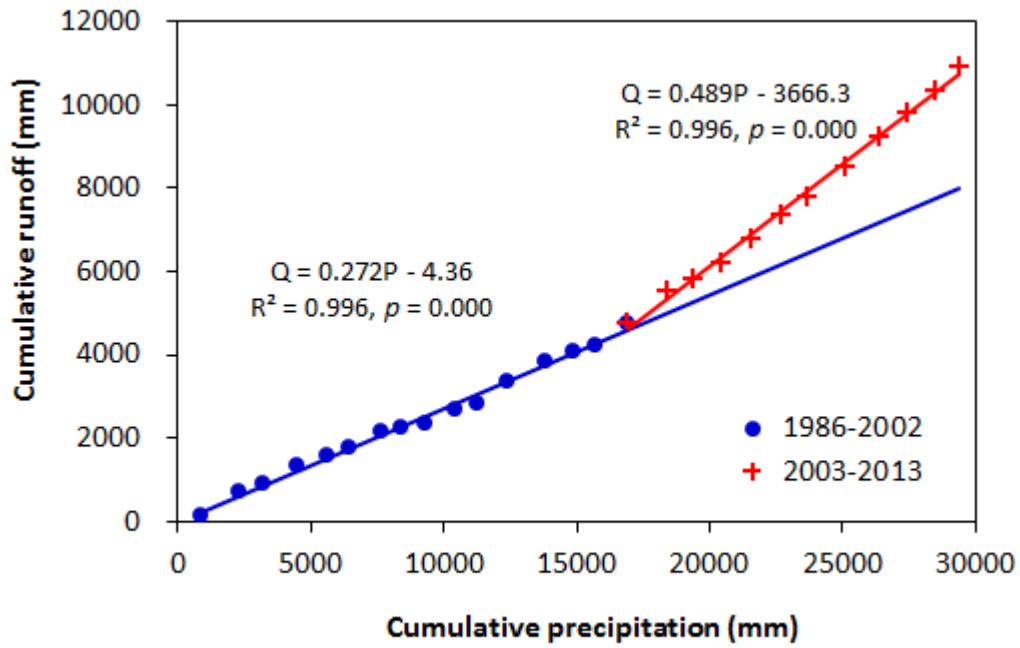


640

641 **Fig. 10.** The trend of monthly groundwater table depth fluctuations measured at the Aiyuan Well
 642 Station in the Lishui subbasin during 2006-2013.

643

644

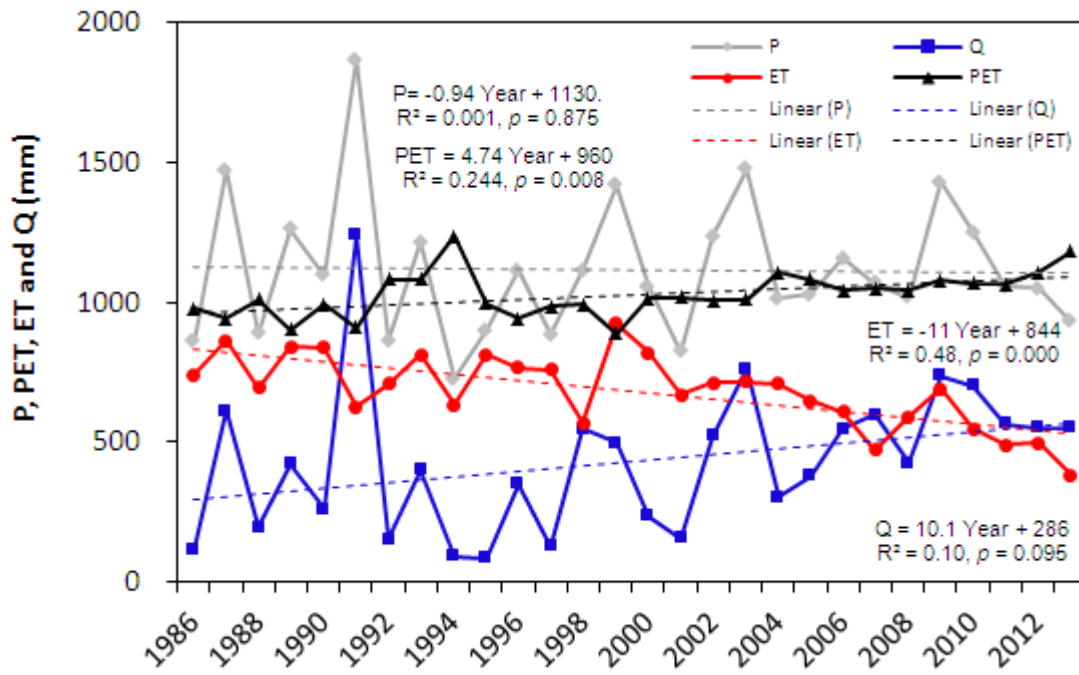


645

646 **Fig. 11.** Double mass curves showing the relationships between accumulated annual precipitation
 647 (P) and total streamflow (Q) for the Qinhuai River Basin (1986-2013). The extreme wet year of
 648 1991 was removed from the analysis.

649

650



651

652

653 **Fig. 12.** Trend of annual water balance and potential evapotranspiration (PET) for the Qinhuai

654 River Basin from 1986-2013. ET was estimated as the difference between precipitation (P) and

655 measured streamflow (Q).

656